

# Capillary electrophoresis of DNA in uncross-linked polymer solutions

Annelise E. Barron\*, David S. Soane and Harvey W. Blanch

Department of Chemical Engineering, University of California, Berkeley, 201 Gilman Hall, Berkeley, CA 94720 (USA)

---

## ABSTRACT

We have used dilute and semi-dilute uncross-linked hydroxyethyl cellulose (HEC) solutions as separation matrices for capillary electrophoresis of DNA restriction fragments. In these experiments, we investigated the effects of HEC molecular weight\* and concentration on resolution, attempting to relate these parameters to the polymer entanglement threshold concentration.

The entanglement thresholds of seven molecular weight fractions of hydroxyethyl cellulose were determined from viscosity-concentration data; the entanglement threshold was found to scale as  $N^{-1.2}$ , where  $N$  = number of HEC monomers. This finding is not in agreement with classical scaling arguments. We present a relationship to predict the observed entanglement threshold of HEC in solution as a function of number average molecular weight.

It was found that excellent separation of  $\Phi$ X174/*Hae*III DNA restriction fragments (72–1353 base pairs) by capillary electrophoresis in HEC solutions can be achieved significantly below the entanglement threshold, depending on DNA size and HEC molecular weight. The mechanism of separation in these uncross-linked polymer solutions must therefore be reexamined. Our experiments show that the entanglement threshold is a useful parameter in predicting a range of HEC concentrations which will separate certain DNA fragments for a given HEC molecular weight. However, the presence of a fully entangled network is not a prerequisite for separation.

---

## INTRODUCTION

Capillary electrophoresis in uncross-linked polymer solutions has been shown to be a promising technique for the rapid and efficient separation of DNA restriction fragments up to 23 000 base pairs (bp) in size [1–6]. While cross-linking a homogeneous and stress-free gel within a capillary can be problematic, the use of uncross-linked polymer solutions enables high-resolution DNA separations to be carried out in an uncoated capillary [4]. Solutions of several different polymers have been employed as separation media for capillary electrophoresis, with varying degrees of success: hydroxyethyl cellu-

lose [4], hydroxypropylmethyl cellulose [2,7], methyl cellulose [1], and polyvinyl alcohol [7], as well as liquified agarose [6,7] and uncross-linked polyacrylamide [3,7]. Solutions of uncross-linked polymers have been found to have separation potential over a wide range of concentrations, from semi-dilute, low-viscosity solutions [4] to extremely concentrated, “syrupy” solutions which are so viscous that they cannot be injected into a capillary and must be polymerized *in situ* [8]. Potentially, the more concentrated solutions have the resolving power to be used for DNA sequencing. It appears that the more dilute solutions will be more suited to mapping and sizing applications, as single base pair resolution for DNA greater than 100 bp in length has not yet been achieved. It has not been established whether the mechanism of DNA separation in an extremely dilute solution is the same as that which occurs in a gel-like, “syrupy” solution. Furthermore, for uncross-linked polymer solu-

---

\* Corresponding author.

\* Upon request of the authors, the term “molecular weight” is used in this paper, rather than the standard “molecular mass” which is preferred in this journal.

tions in general, the relationship between the resolution and the molecular weight and concentration of the polymer is not yet fully understood. No theory exists to accurately predict the appropriate polymer size and concentration for a desired separation.

The mechanism of DNA separation in uncross-linked polymer solutions continues to be a matter of controversy. Some groups have asserted that the mechanism is essentially the same as that in traditional slab gel electrophoresis [2,4], while others attribute separation to the attraction and interaction of DNA fragments with the cellulose derivatives in the buffer [1,5]. Still others have theorized that the separation involves a mechanism of exclusion from the polymer fiber network similar to that occurring in gel permeation chromatography [9].

We address these questions both experimentally and theoretically, employing hydroxyethyl cellulose (HEC) solutions as a separation matrix for capillary electrophoresis. We discuss the structural characteristics which allow solutions of HEC (and other cellulosic polymers) to act as an effective separation matrix for electrophoresis of DNA. In fact, the mechanism of DNA separations in dilute and semi-dilute uncross-linked HEC solutions may involve entanglement coupling between the DNA and the uncross-linked HEC. We present the results of rheological and capillary electrophoresis experiments with several different molecular weights of HEC, and present evidence that for fine resolution, the average distance between entanglement points in the HEC solution must be approximately equal to the contour length of the DNA molecules of interest.

## BACKGROUND AND THEORY

### Structure of hydroxyethyl cellulose

Cellulose is a naturally occurring high polymer in which  $\beta$ -D-glucopyranoside units are condensed through a 1,4'-linkage to form a linear molecule. HEC is a hydrophilic cellulose derivative, synthesized commercially by reacting alkali cellulose with ethylene oxide at high temperatures [10]. Substitution may be expressed in terms of the moles of ethylene oxide per

anhydroglucose unit, designated as the molar substitution (M.S.). On average, HEC has an M.S. of 2.5, giving an average monomer molecular weight of 272 g/mol. A typical structural element of the HEC molecule is shown in Fig. 1.

### Properties of HEC in solution

The dissolution of HEC in water is accomplished by the expansion of the structure by the bulky substituent groups, especially the polyethylene oxide side chains which terminate in the hydrophilic hydroxyethyl group [10]. Cellulose derivatives such as HEC are known to be highly extended and inflexible in solution. While a typical non-cellulosic polymer has a Porod-Kratky persistence length of only 0.8–1.0 nm, that of HEC in water has been estimated at 8.3 nm [10]. Stiff and extended molecules are known to exhibit more pronounced effects of entanglement than highly flexible polymers [11]. The experiments of Saunders *et al.* [12] show that for cellulosic polymers the presence of bulky side chains, such as the bulky ethylene oxide group in HEC, does not significantly affect the onset of entanglement coupling. Thus, it is thought that these stiff, extended molecules form an entangled network through a long-range looping of chains, rather than through short-range interactions such as local kinks [13]. Fig. 2 is a schematic representation of this type of long-range looping. Although a mesh formed by long-range interactions of inflexible, extended HEC

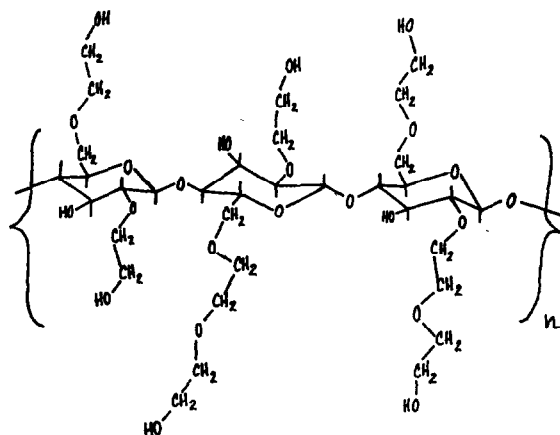


Fig. 1. A typical structural element of a hydroxyethyl cellulose chain (three monomers shown).

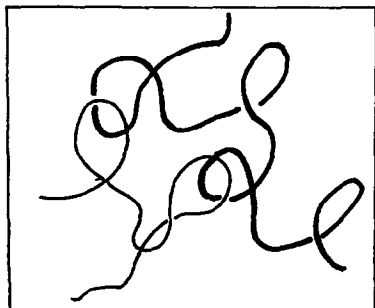


Fig. 2. Long-range entanglement coupling between two polymers. Since the presence of bulky side-groups, like the ethylene oxide group of HEC, does not inhibit the onset of entanglement coupling in solutions of cellulosic polymers, it seems likely that these interactions involve long-range looping rather than short-range kinking or knotting [12].

molecules will be fairly stiff, it will not be tightly “knotted” and therefore will have a dynamic structure.

#### *Entanglement coupling between HEC and DNA*

It is important to note that DNA molecules can also be described as stiff and extended in solution, even more so than HEC. In fact, the Porod–Kratky persistence length of double-stranded DNA is about 45 nm at an ionic strength of 0.2 M [14]. Therefore, it is likely that DNA experiences some degree of entanglement coupling with HEC molecules in solution, the effects of which are augmented by the stiffness of the two participants in the interaction. This entanglement coupling, theoretically, could sufficiently alter the frictional characteristics of the DNA molecules moving under the influence of the electric field so as to render size-dependent separations possible. This mechanism of separation is quite different from that postulated to occur in cross-linked polyacrylamide or agarose gels.

Consider the frictional characteristics of a molecule when no entanglement coupling is present. Einstein showed that in general, for large particles,

$$D = \frac{kT}{(\text{molecular friction factor})} \quad (1)$$

where  $D$  is the diffusion coefficient,  $k$  is Boltzmann’s constant,  $T$  is the temperature, and

the “molecular friction factor” is defined as the force required to pull the undeformed molecule through its surroundings at unit velocity [15]. It has been demonstrated by Bueche [16] that this molecular friction factor is strongly affected by entanglement coupling, and the following discussion closely follows his work.

Consider a freely orienting polymer, consisting of  $N$  subunits, that is not entangled with other polymers. If a force  $f_0$  is needed to pull a single freely orienting segment through its surroundings at unit velocity, then the total frictional coefficient for the non-entangled polymer is  $Nf_0$ , where  $f_0$  is a “segmental friction factor.” Substitution of this relationship into eqn. 1 gives

$$D = \frac{kT}{Nf_0} \quad (\text{no entanglements}) \quad (2)$$

Now, consider a polymer molecule which is entangled with other polymer molecules in solution. In this case, a force larger than  $Nf_0$  is required to pull the polymer through the solution at unit velocity. Assume that all of the polymer molecules are identical and that entanglement points exist at uniform distances along a molecule, where  $L_e$  is the average molecular contour length between entanglement points.

If a particular molecule, the primary molecule, is pulled along at unit velocity, a force  $Nf_0$  is required to pull its constituent segments through solution. A number of other molecules will be entangled with the primary molecule in such a way as to slow its progress (see Fig. 3). Since these molecules are not firmly attached to the primary molecule, they will slip as the primary



Fig. 3. A schematic representation of the entanglement coupling interaction of DNA, moving under the influence of an electric field, with the HEC molecules in the buffer.

molecule moves through solution. They will be transported at some velocity which is less than the velocity of the primary molecule.

In turn, those molecules which are entangled with the primary molecule will pull with them still other molecules; these molecules will pull with them still other molecules, and so on. The net effect of these entanglement couplings is to require the application of a force much larger than  $Nf_0$  if the primary molecule is to be pulled through solution at unit velocity. Furthermore, this increase in the molecular friction factor will be dependent on  $N$ , the number of polymer segments; for the longer the polymer is, the more entanglement points which will exist, and the slower the polymer will progress through solution. Indeed, this behavior is observed in the capillary electrophoresis of DNA in entangled polymer solutions, where electrophoretic mobility decreases with increasing size [4]. This general trend, however, is the same when DNA is electrophoresed in a cross-linked gel, which has an interconnected system of semi-rigid pores. In order to show that the mechanism is different, we must show that good separations can occur before the separation matrix in the buffer is fully entangled; *i.e.*, before any porous network-like structure could exist.

#### Determination of entanglement threshold

The *entanglement threshold* ( $\Phi^*$ ) is defined as the concentration at which polymer molecules begin to overlap and interact strongly in solution. This critical concentration has been identified as the point at which *network formation* through chain entanglement becomes possible; *i.e.*, below  $\Phi^*$  there may be some entanglement coupling between isolated molecules, but it does not extend throughout the system [17].

Experimentally, the concentration at which polymer chains in a given narrow molecular weight range form an entangled network can be determined from a log–log plot of specific viscosity ( $\eta_{sp}$ ) vs. polymer weight fraction ( $\Phi$ ). At low concentrations ( $\Phi < \Phi^*$ ), where the polymer molecules do not interact extensively in solution, specific viscosity is linear with concentration. At the entanglement threshold ( $\Phi \approx \Phi^*$ ), the  $\eta_{sp}$  vs.  $\Phi$  data exhibit a break and an

increase in slope, since the presence of an entangled polymer network makes a large contribution to solution viscosity [18].

For any given polymer,  $\Phi^*$  will have a unique dependence on molecular weight. DeGennes [19] recognized that  $\Phi^*$  was an essential scaling parameter, and used polymer physics to derive a scaling relationship between  $\Phi^*$  and molecular weight. This expression is based on the assumption that when  $\Phi \approx \Phi^*$ , the bulk concentration of the solution is the same as the concentration inside a single coil. For randomly coiling polymers in an athermal solvent, it follows that

$$\Phi^* \sim N^{-0.8} \quad (3)$$

where  $N$  is the number of monomer units. This expression states that  $\Phi^*$  scales as  $N^{-0.8}$ , but in order to use this relationship in a predictive fashion, one must know the coefficient and additive constant. To this end, in our study of HEC we compared the molecular weight dependence of the entanglement threshold with that predicted by deGennes. We did not expect perfect agreement with this scaling relationship, since (1) HEC is stiff and extended in solution and therefore deviates appreciably from the model of a random coil, and (2) water is a good solvent for HEC, not an athermal solvent.

#### Average mesh size of an entangled network

In addition, deGennes [19] assumed that at polymer concentrations above the entanglement threshold, an entangled network of polymers could be characterized with an “average mesh size,” designated  $\xi$ . He assumed first that for  $\Phi > \Phi^*$ ,  $\xi$  depends only on  $\Phi$  and not on the number of monomer units in the chain; *i.e.*, the average mesh size is less than the contour length of the polymer. Secondly, he assumed that when  $\Phi \approx \Phi^*$ , the mesh size is about the same as an individual polymer coil ( $R_g$ ). With these assumptions the following scaling relationship was obtained:

$$\xi(\Phi) \sim a\Phi^{-0.75} \quad (\Phi^* < \Phi < 1) \quad (4)$$

where the units of  $\xi$  are nanometers, and  $a$  is the statistical segment length of HEC, a constant tabulated as 0.425 nm [20]. Once again, how-

ever, this is simply a *scaling* relationship, and no direct or approximate equality is implied. It was suggested by Grossman and Soane [4] that since combining eqns. 3 and 4 leads to the relationship  $\xi(\Phi^*) \sim aN^{0.60}$ , it should be possible to tailor the mesh size at  $\Phi^*$  simply by using the correct HEC length.

#### The average molecular contour length between entanglement points

It is interesting to compare the scaling of the average mesh size discussed above, a concept which is only meaningful for a fully entangled mesh, to the average molecular contour length between entanglement points ( $L_e$ ), a meaningful quantity both above and below the entanglement threshold.  $L_e$  provides a means of describing entanglement interactions which may occur at concentrations *below*  $\Phi^*$ . Once again drawing from the work of Bueche [16], we can derive the scaling relationship between  $L_e$  and the concentration of polymer in solution ( $\Phi$ ). In fact,  $L_e$  will be inversely proportional to  $\Phi$ . This becomes obvious if one considers that one can dilute a highly entangled network of polymers with a good solvent until the polymer concentration in solution is so low that molecules no longer overlap, and no entanglements between molecules will exist. It follows that  $L_e$  will increase as  $\Phi$  decreases. There will be concentrations below the entanglement threshold where transient entanglement coupling between individual molecules occurs, so that on average  $L_e$  will be only slightly less than the contour length of the polymer molecule. Thus,  $L_e$  can take on a continuum of values, both below and above the entanglement threshold.

This concentration dependence of  $L_e$  can be justified more rigorously. Consider a polymer molecule in solution which is looped around itself in several places, so that if another polymer molecule passed through one of these loops it could form a point of entanglement. The number of other polymer molecules passing through one of these loops will be proportional to the total concentration of polymers in solution,  $\Phi$  [16]. Thus, the probability that a given loop in a polymer is entangled with another polymer is proportional to  $\Phi$ . Since  $L_e$  equals the total

contour length of the polymer divided by the number of entanglement points, it follows that  $L_e \sim 1/\Phi$ . This leads to the relationship

$$L_e \Phi = \text{constant} \quad (5)$$

This equation assumes that a given polymer in an entangled network always has more possible points along its length where other entanglements *could* occur, if the concentration of polymer in solution were greater. Due to steric hindrances and other factors, the number of possible entanglement points per molecule probably reaches some asymptotic value at high concentrations which is related to its structure.

At the entanglement threshold, the average mesh size given in eqn. 4 should be comparable to the average contour length between entanglements. However, an additional relationship is required to make this comparison. This is provided by Ferry [21], who states that at the entanglement threshold there must be on average two entanglement points per molecule. By analogy with the theory of cross-linked gels, the entanglement coupling may extend throughout the system if, statistically, each molecule has two entanglement points. In other words, at the entanglement threshold,

$$L_c = 2L_e \quad (\Phi = \Phi^*) \quad (6)$$

where  $L_c$  is the average total contour length of the polymer molecule, a quantity which may be calculated easily, given knowledge of the number-average molecular weight ( $M_n$ ), monomer molecular weight ( $M_0$ ), and the monomer dimensions ( $L_m$ ):

$$L_c = \left( \frac{M_n}{M_0} \right) L_m \quad (7)$$

Combining eqns. 5, 6 and 7, one arrives at the relationship

$$\Phi^* \sim M_n^{-1} \quad (8)$$

Since the number of monomers ( $N$ ) can be calculated by dividing  $M_n$  by the monomer molecular weight ( $M_0$ ), Eqn. 8 is equivalent to stating that  $\Phi^* \sim N^{-1}$ , which is different from deGennes' [19] result in eqn. 3. We have determined  $\Phi^*$  for several different molecular

weights of HEC in order to compare experimental results with the predictions of eqns. 3 and 8.

## EXPERIMENTAL

### Instrumentation

The capillary electrophoresis apparatus used in these studies employs a straight length of fused-silica capillary with an external coating of polyimide (Polymicro Technologies, Phoenix, AZ, USA) and no internal coating, 50 cm in length (35 cm to the detector), with 51  $\mu\text{m}$  I.D. and 360  $\mu\text{m}$  O.D. The capillary connects the anodic reservoir with the electrically grounded cathodic reservoir. A high-voltage power supply with a 30 000-V capacity (Gamma High Voltage Research, Ormand Beach, CA, USA) was used to drive electrophoresis. Current was measured over a 1-k $\Omega$  resistor in the return circuit of the power supply, using a digital multimeter (Model 3465B, Hewlett-Packard, Palo Alto, CA, USA). On-column detection was by UV absorbance at 260 nm, using a modified variable-wavelength detector (Model 783, Applied Biosystems, Foster City, CA, USA). Data were collected using an integrator (Model 3390, Hewlett-Packard).

### Materials

A  $\Phi\text{X174}/\text{HaeIII}$  restriction digest was obtained from Bethesda Research Labs (Bethesda, MD, USA). Mesityl oxide was used as a neutral marker (Aldrich, Milwaukee, WI, USA). The buffer used in all experiments was 89 mM tris(hydroxymethyl)aminomethane (Tris) and 89 mM boric acid, with 5 mM ethylenediaminetetraacetic acid (EDTA) added as a chelating agent, pH 8.15 (all buffer reagents purchased from Sigma Molecular Biology, St. Louis, MO, USA). Varying amounts of hydroxyethyl cellulose (HEC) were added to buffer solutions; mixtures were vigorously shaken and then mixed for 24 h by tumbling (mixing by mechanical stirring sometimes led to incomplete dissolution). Seven different (number-average) molecular weight fractions of HEC were used: samples with molecular weight ranges of  $M_n \approx 24\ 000$ – $27\ 000$ ,  $M_n \approx 90\ 000$ – $105\ 000$ , and  $M_n \approx 140\ 000$ – $160\ 000$  g/mol were obtained from Polysciences (War-

ington, PA, USA). (Hereafter these samples will be referred to as  $M_n\ 27\ 000$ ,  $M_n\ 105\ 000$ ,  $M_n\ 160\ 000$ , for brevity.) Samples with average molecular weights  $M_n \approx 35\ 900$ ,  $M_n \approx 63\ 800$ ,  $M_n \approx 306\ 000$  and  $M_n \approx 438\ 800$  were donated by the Aqualon (Wilmington, DE, USA) and were designated as Natrosol 250L, 250EXR, 250MR, and 250H, respectively. The average molecular weights of these Natrosol products were previously determined by Sperry [22] using intrinsic viscosity measurements. The molecular weight ranges of the HEC samples from Polysciences were determined by the company. The ratio of weight-average molecular weight to number-average molecular weight (a measure of sample polydispersity) has not yet been measured for these HEC samples.

### Methods

**Capillary zone electrophoresis.** Before each experiment, the uncoated inner capillary wall was conditioned first with 1 M NaOH for 10 min, then with 0.1 M NaOH for 10 min, and finally with the electrophoresis buffer (containing dissolved HEC) for 20 min. The electric field was turned on and left on until current through the capillary had stabilized, usually 10–15 min. Buffer solutions were degassed immediately prior to use. Samples were introduced to the anodic end of the capillary by applying a vacuum of 4 inch Hg (13546 Pa) for a specific time which depended on the buffer viscosity, so as to introduce approximately 3 nl ( $3 \cdot 10^{-6}$  cm<sup>3</sup>) of sample for each run. After the sample slug was drawn into the capillary, the anodic end of the capillary was placed back into the electrophoresis buffer, together with the anodic electrode, and the electrophoretic voltage was applied. All experiments were run at 11 kV (220 V/cm). The capillary was surrounded by agitated air at a temperature of  $30.0 \pm 0.1^\circ\text{C}$  in all experiments.

Note that DNA, which is negatively charged, would remain at the anodic end of the capillary were it not drawn toward the UV absorbance detector and the cathode by strong electroosmotic flow. Thus, the largest DNA fragment, which has the smallest electrophoretic mobility in the direction of the anode, will pass the detector first, followed by the smaller ones in

order of size. A description of the method used to calculate electrophoretic mobilities can be found elsewhere [23]. The capillary electrophoresis apparatus used in these studies is configured in such a way that electrokinetic injection at the cathode is difficult; because of this limitation, hydrodynamic injection at the anode required that uncoated capillaries, which engender strong electroosmotic flow, be used to drive the DNA past the detector.

Each new, uncoated capillary was treated with 1 M NaOH for three hours before performing the first run, to etch the fused-silica surface completely clean. After the initial 3-h treatment with 1 M NaOH, 10-min treatments with base between runs sufficed to clean out the previous buffer-HEC mixture and refresh the necessary wall condition for excellent separations.

**Viscosity measurements.** Viscosity measurements were performed with an Ostwald viscometer which had been previously characterized with two viscometer constants,  $\alpha$  and  $\beta$  [18]. Previous experiments with HEC in water have shown that the effect of shear rate on viscosity may be neglected [10]. Densities of the HEC-buffer solutions were determined by weighing sample volumes of 25 cm<sup>3</sup> at room temperature. During all experiments the viscometer was thermostatted in a water bath at 25.0 ± 0.1°C.

## RESULTS AND DISCUSSION

### Determination of entanglement threshold

The entanglement threshold,  $\Phi^*$ , was determined for seven molecular weight fractions of HEC, shown in Table I. Since in our comparison with theoretical entanglement threshold scaling the important parameter is the *number of monomers*, it is appropriate to use the *number-average* molecular weight, a measure of the average number of repeat units per polymer molecule, rather than the viscosity-average molecular weight or the weight-average molecular weight [24]. Fig. 4 shows a representative plot of  $\log \eta_{sp}$  vs.  $\log \Phi$  used to determine  $\Phi^*$  for each HEC molecular weight. In each case,  $\Phi^*$  was taken to be the point at which the data begin to deviate significantly from a straight line. Table I summarizes the values of  $\Phi^*$  [as % (w/w) HEC in

TABLE I

### EXPERIMENTALLY DETERMINED ENTANGLEMENT THRESHOLDS

$M_n$  = Number-average molecular weight of HEC.  $\Phi^*$  = Entanglement threshold, weight percent HEC in buffer.

$M_n$ (g/mol)	$\Phi^*$ (% w/w)
27 000	1.80
35 900	1.25
63 800	0.68
105 000	0.37
160 000	0.21
306 000	0.11
438 800	0.09

buffer solution for each HEC molecular weight. It is important to note that this measured entanglement threshold reflects the concentration at which an infinite entangled *network* begins to form; below this concentration, an individual HEC molecule has, on average, less than two points of entanglement [21].

The number of monomers,  $N$ , was calculated by dividing the number-average molecular weight by the monomer molecular weight of HEC (M.S. = 2.5) of 272 kg/kmol. If we plot  $\log \Phi^*$  vs.  $\log N$  (Fig. 5), we see that  $\Phi^*$  scales as  $N^{-1.2}$  rather than  $N^{-0.8}$  as deGennes [19] predicts in eqn. 3 or as  $N^{-1.0}$  as Bueche predicts in eqn. 8 [16]. Thus, the onset of entanglement is a stronger function of molecular weight for HEC than that predicted for a randomly coiling poly-

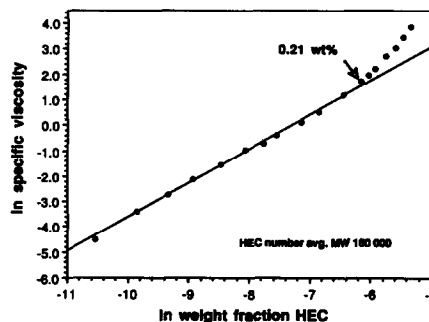


Fig. 4. A representative plot of the logarithm of the specific viscosity vs. the logarithm of HEC weight fraction, used to find the entanglement threshold ( $\Phi^*$ ) for each HEC molecular weight. In this case, the HEC has a number average molecular weight of 160 000 g/mol.

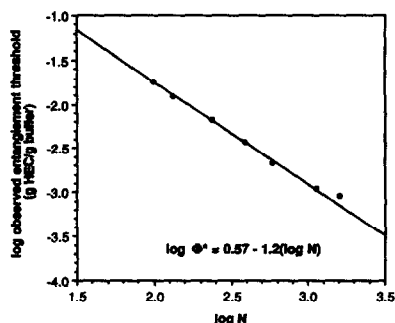


Fig. 5. A plot of the logarithm of the entanglement threshold (g HEC/g buffer) vs. the logarithm of the number of HEC monomers in the chain, showing that  $\Phi^*$  scales as  $N^{-1.2}$ .

mer, consistent with the known stiffness of HEC in solution. Fig. 6 shows a plot of  $\Phi^*$  vs.  $N^{-1.2}$ ; the data are a good fit to a line with a positive intercept at  $1.18 \cdot 10^{-4}$  g HEC/g buffer. Thus, a solution of “infinitely” long HEC molecules would be entangled even at this low concentration. Furthermore, the following relationship may be used to predict entanglement threshold for any HEC molecular weight fraction for which the number-average molecular weight is known:

$$\Phi^* = 3.63 \left[ \frac{M_n}{M_0} \right]^{-1.2} + 1.18 \cdot 10^{-4} \quad (9)$$

where  $\Phi^*$  is measured as g HEC/g solvent and  $M_0$  is the average monomer molecular weight, which will vary with the molar substitution (M.S.). Most HEC has an M.S. of 2.5, which gives an  $M_0$  of 272 g/mol.

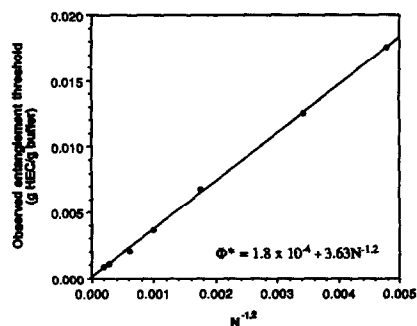


Fig. 6. A plot of the entanglement threshold ( $\Phi^*$ ) vs.  $N^{-1.2}$ . Note that the line which fits this data has a positive intercept of  $1.18 \cdot 10^{-4}$ .

### Capillary electrophoresis experiments

We wished to test the importance of the entangled network of HEC chains in DNA separations; specifically, whether a definite mesh-like structure in HEC solutions is necessary for DNA separation. It has been proposed by Grossman and Soane [4] that this entangled network plays the same role as a cross-linked gel network in the electrophoretic separation of DNA restriction fragments, *i.e.*, that the mechanism of separation was essentially the same in cross-linked and uncross-linked sieving matrices. In our experiments, however, we found that the existence of a fully entangled network is not a necessary condition for separation. That is, an HEC solution used to fill an uncoated capillary

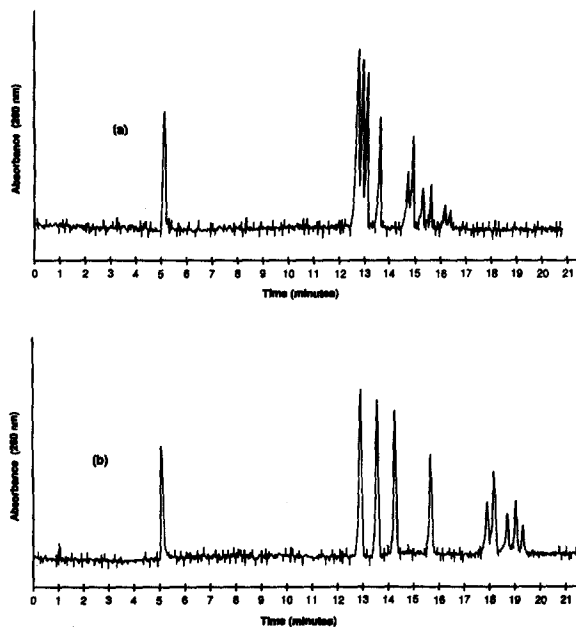


Fig. 7. Capillary electrophoresis of eleven  $\Phi$ X174/*Hae*III restriction fragments ranging in size from 72 to 1353 bp in (a) 0.35% (w/w)  $M_n$  27 000 HEC, and (b) 0.09% (w/w)  $M_n$  105 000 HEC, both in 89 mM Tris–89 mM boric acid–5 mM EDTA. Reading from left to right (not including the first peak, which is a neutral marker), the species are (a) 1353, 1078, 872, 603, 310, 281 + 271, 234, 194, 118, and 72 bp in length, and (b) 1353, 1078, 872, 603, 310, 281 + 271, 234, 194 + 118, 72 bp in length, respectively. Conditions: field strength 221.4 V/cm; current (a) 7.2  $\mu$ A, (b) 7.1  $\mu$ A; UV detection at 260 nm; capillary dimensions, 50 cm total length (35 cm to detector)  $\times$  51  $\mu$ m I.D.; temperature,  $30 \pm 0.1^\circ$ C. R.S.D. of absolute electrophoretic mobilities: (a) 0.21%,  $n = 5$ ; and (b) 0.37%,  $n = 6$ .



may be at a concentration significantly below its entanglement threshold and still well separate DNA restriction fragments. Fig. 7a shows the electrophoretic separation of  $\Phi$ X174/*Hae*III restriction fragments in a buffer containing 0.35% (w/w)  $M_n$  27 000 HEC. HEC of this molecular weight does not form an entangled network at concentrations below 1.8% (w/w). (In all electropherograms, peak heights are attenuated by a factor of 4.0.) In Fig. 7b the same restriction digest is separated in buffer containing 0.09% (w/w)  $M_n$  105 000 HEC, although the entanglement threshold of this HEC fraction is 0.37% (w/w). Similar examples could be cited for electrophoresis in buffer solutions containing HEC of molecular weights up to  $M_n$  438 800. UV absorbance peaks for the  $\Phi$ X174/*Hae*III restriction fragments were identified from integrated peak areas, as shown in Fig. 8 by a representative plot of peak area vs. number of base pairs.

The question could be raised as to whether the solution within the capillary is homogeneous in concentration, *i.e.*, whether HEC adsorption on the capillary walls perhaps creates local regions with HEC concentration higher than the bulk concentration. If this were the case, concentrations near the wall could be *above* the entanglement threshold of the solution, although the bulk solution is well below this concentration. Our experiments show that this is probably not the case. Since we were constrained to use uncoated capillaries with our apparatus (see

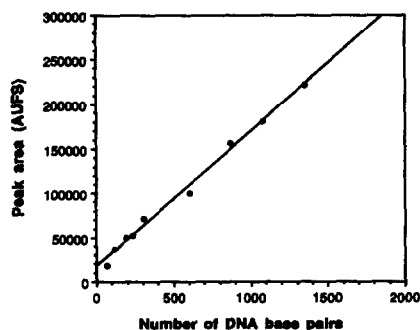


Fig. 8. A representative plot of UV absorbance peak area vs. number of DNA base pairs. This particular plot was obtained for electrophoresis at 220 V/cm of  $\Phi$ X174/*Hae*III restriction fragments in a buffer containing 0.22% (w/w)  $M_n$  105 000 HEC.

*Methods*), and we etched the capillary walls with strong base prior to each replacement of the HEC–buffer solution, the  $\zeta$  potential of the capillary wall was quite high, even in the presence of HEC–buffer solution. This is evidenced by the strong electroosmotic flow in our experiments (a neutral marker typically eluted after about five minutes at a field strength of 220 V/cm). Were the HEC strongly adsorbed to the wall, or adsorbed in thick layers, negative charges on the wall would be effectively shielded and electroosmotic flow would be much reduced. Also, if the concentration profile within the capillary were inhomogeneous, with a higher concentration of HEC near the wall, DNA molecules near the wall would experience different amounts of sieving than those in the center of the capillary, and peaks would be broadened. But it can be seen that even in Fig. 7a, where the HEC concentration is well below the entanglement threshold and DNA separation definitely occurs, that peaks are quite sharp. Since peaks are sharp and electroosmotic flow is strong, since buffer pH is high (pH 8.2), and since temperature is also relatively high (30°C), there is more likely a rapid adsorption/desorption process which leads to ineffective shielding of the negative charges on the wall and a homogeneous concentration within the capillary.

However, an investigation needs to be conducted into the importance of electroosmotic flow and the condition of the capillary walls on the success of DNA separations in uncoated capillaries in dilute HEC solutions. Note that at typical fields, with DNA injection at the anodic end of the capillary, electroosmotic mobility is *twice* the electrophoretic mobility of the DNA, and opposite in direction. This situation may be quite different from that of a DNA molecule moving through a stagnant solution. Work is proceeding in our laboratory now to reproduce these separations in a *coated* capillary with no electroosmotic flow.

It was clear from our experiments that the HEC length strongly affected the “window of DNA separation,” that is, the size range of the restriction fragments which could be separated with good resolution. In general, the larger HEC molecular weights ( $M_n$  105 000, 160 000, 306 000,

and 438 800 HEC) could well separate the larger  $\Phi$ X174/*Hae*III fragments (1353, 1078, 872, and 603 bp) within a certain concentration range which was specific to each HEC molecular weight. Generally, above a certain minimum HEC concentration (unrelated to the entanglement threshold), the larger DNA fragments were better resolved at *low* HEC concentrations. The smaller HEC, on the other hand, did not resolve these larger DNA fragments well even at low concentrations, and could not resolve them at all above a certain HEC concentration. This is illustrated by the electropherogram in Fig. 9a, in which  $\Phi$ X174/*Hae*III restriction fragments are separated in a buffer containing 0.95% (w/w)  $M_n$  35 900 HEC. From these results we conclude that the mechanism of separation is related to the relative sizes of the DNA and HEC. We postulate that if the HEC molecules are too small, in their interactions with these larger DNA restriction fragments they are unable to

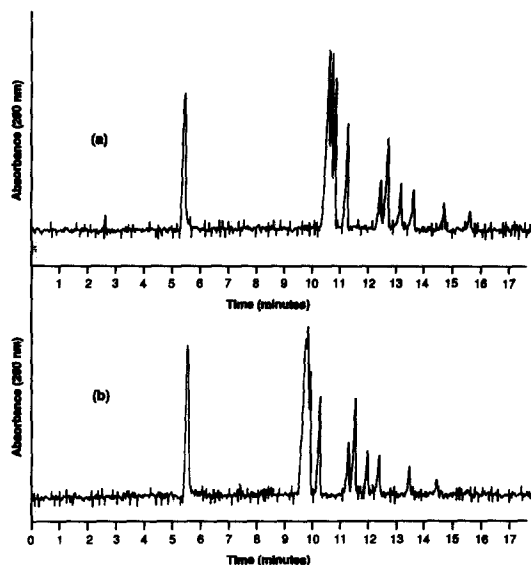


Fig. 9. Capillary electrophoresis of  $\Phi$ X174/*Hae*III restriction fragments ranging in size from 72 to 1353 bp in (a) 0.95% (w/w)  $M_n$  35 900 HEC, and (b) 1.35% (w/w)  $M_n$  35 900 HEC, both in 89 mM Tris–89 mM boric acid–5 mM EDTA. Reading from left to right (not including the first peak, which is a neutral marker), the species are 1353, 1078, 872, 603, 310, 281 + 271, 234, 194, 118, and 72 bp in length, respectively. Conditions: field strength 221.4 V/cm; current (a) 8.8  $\mu$ A, (b) 9.3  $\mu$ A; UV detection at 260 nm; capillary dimensions, 50 cm total length (35 cm to detector)  $\times$  51  $\mu$ m I.D.; temperature,  $30 \pm 0.1^\circ\text{C}$ . R.S.D. of absolute electrophoretic mobilities: (a) 1.16%,  $n = 5$ ; and (b) 0.93%,  $n = 7$ .

form the firm entanglements that will significantly hinder DNA electrophoretic motion, and thus they are unable to introduce a size-dependence to the DNA molecular friction factor.

Considering the separation shown in Fig. 9a once again, we remark that this is still below the entanglement threshold for this polymer [1.25% (w/w)], and that the only fragments which are not resolved in this 11-fragment mixture are the 271/281 bp fragments. [We note that it is likely that with smaller sample volumes (*i.e.*, less than 3 nl) and a more sensitive method of detection, such as fluorescence, better resolution of these fragments could be achieved; however, we are interested only in the *relative* performance of our apparatus at different HEC concentrations, as it reflects on the mechanism of DNA separation.] If the concentration of this  $M_n$  35 900 HEC is increased beyond the entanglement threshold the 271/281 bp fragments remain unresolved, and in fact resolution of the larger fragments declines, as shown in Fig. 9b with  $M_n$  35 900 HEC at 1.35% (w/w). It is interesting that resolution of the larger DNA fragments is almost completely lost when the concentration of HEC is increased. If one was attempting to explain the results in terms of conventional gel electrophoresis models, one might expect, as the HEC network tightened, that the larger DNA fragments would enter the reptation regime, in which the electrophoretic mobility scales as  $1/N$ . If the larger DNA fragments began to reptate, resolution would *improve* as the HEC network tightened. Since this does not occur, we postulate that perhaps reptation cannot occur these dilute uncross-linked solutions, since there are no semi-rigid pores to force the DNA to take a tortuous path. Instead, once the solution reaches a high enough concentration to confine the motion of the larger DNA to an “effective tube,” it moves immediately in the biased reptation regime, moving through the solution at a steady-state velocity independent of DNA length. This may be because confining the range of motion of the DNA makes it less probable that entanglement coupling with HEC can occur; yet since the tube “walls” are not semi-rigid like those of a gel, but are probably dilating on a time scale much shorter than the DNA residence time in this tube, neither is the DNA forced to follow a

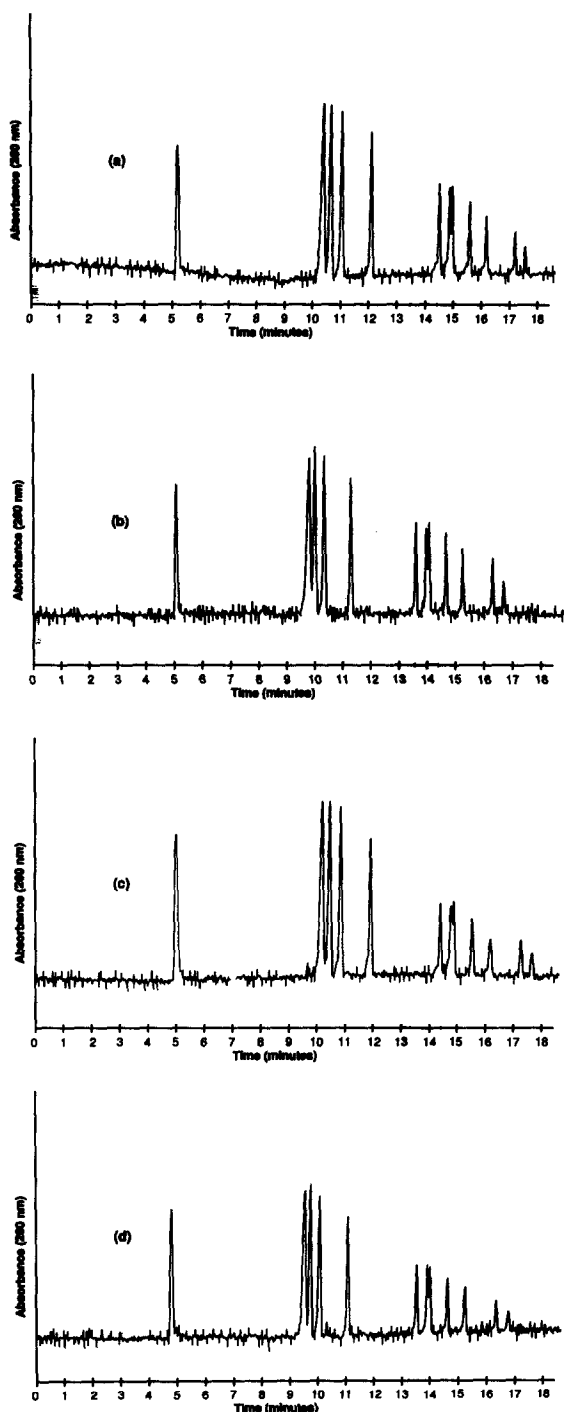


Fig. 10. Capillary electrophoresis of  $\Phi$ X174/*Hae*III restriction fragments ranging in size from 72 to 1353 bp in (a) 0.225% (w/w)  $M_n$  105 000 HEC, (b) 0.225% (w/w)  $M_n$  160 000 HEC, (c) 0.22% (w/w)  $M_n$  306 000 HEC, (d) 0.225% (w/w)  $M_n$  438 800 HEC, all in 89 mM Tris–89 mM boric acid–5 mM EDTA. Reading from left to right (not including

tortuous path. We have not considered here concentrated HEC solutions [i.e., above 2% (w/w)]; it is possible that when HEC concentration is high enough, the network may become stiff and confining, allowing DNA reptation to occur as it is postulated to occur in rigid, cross-linked gels. While it is certain that a striking difference in structure and motion exists between a dilute, uncross-linked polymer solution and a semi-rigid cross-linked gel, there may be very little difference between an extremely concentrated, “syrupy” polymer solution and the aforementioned gel.

We note as well that Beebe-Poli and Schure [25] performed capillary electrophoresis in uncross-linked HEC, separating different lengths of poly(styrenesulfonate), a stiff, rod-like polymer which is negatively charged in proportion to its length, like DNA. These workers concluded after extensive analysis of their data that the mechanism of separation was neither Ogston-type sieving nor reptation, and that in fact conventional electrophoresis theories could not model their data.

We found that neither the  $M_n$  27 000,  $M_n$  35 900, nor the  $M_n$  63 800 HEC was capable of separating the 271/281 bp fragments at any concentration above or below the entanglement threshold, even when the capillary was loaded with sample volumes less than 2 nl. However, an interesting finding is that the 271/281 bp fragments can be separated in uncross-linked HEC solutions, using the same larger HEC molecular weights that separate large restriction fragments well ( $M_n$  105 000,  $M_n$  160 000,  $M_n$  306 000, and  $M_n$  438 800 HEC). This is illustrated in Fig. 10a [0.225% (w/w)  $M_n$  105 000 HEC], Fig. 10b [0.225% (w/w)  $M_n$  160 000 HEC], Fig. 10c [0.22% (w/w)  $M_n$  306 000 HEC], and Fig. 10d [0.225% (w/w)  $M_n$  438 800 HEC]. Since we found that for these dilute solutions these two fragments could only be separated in a narrow

the first peak, which is a marker), the species are 1353, 1078, 872, 603, 310, 281, 271, 234, 194, 118, and 72 bp in length, respectively. Conditions: field strength 221.4 V/cm; current (a) 7.1  $\mu$ A, (b) 7.1  $\mu$ A, (c) 7.4  $\mu$ A, (d) 7.3  $\mu$ A; UV detection at 260 nm; capillary dimensions, 50 cm total length (35 cm to detector)  $\times$  51  $\mu$ m I.D.; temperature,  $30 \pm 0.1^\circ$ C. R.S.D. of absolute electrophoretic mobilities: (a) 0.30%,  $n=7$ ; (b) 0.24%,  $n=6$ ; (c) 0.23%,  $n=5$ ; and (d) 0.81%,  $n=7$ .

concentration range of HEC in the buffer [ $\pm 0.05\%$  (w/w)], it is striking that optimum resolution is at about 0.22% (w/w) for all four HEC molecular weights which can separate them.

The concept of the contour length between entanglements ( $L_e$ ) can be used to attempt an explanation of this. Recall Ferry's assertion [11] that on average,  $L_c = 2L_e$  at the entanglement threshold (eqn. 6). It is known that the dimensions of HEC in water are 0.519 nm per anhydroglucose unit [10]. Thus,  $L_e(\Phi^*)$  can be determined for all seven HEC molecular weight fractions used in this study, and compared to the contour lengths of the restriction fragments of interest (Table II). Assuming 0.34 nm per base pair [14], DNA restriction fragments of 271 and 281 bp are 92.1 and 95.5 nm in length, respectively. Consider in particular the value of  $L_e(\Phi^*)$  for  $M_n$  160 000 HEC. For  $M_n$  160 000 HEC, the entanglement threshold [0.21% (w/w)] is quite near the concentration of interest [0.22% (w/w)]. It can be seen in Table II that  $L_e(\Phi^*)$  is equal to about 150 nm, somewhat longer than the 271/281 bp fragments. Slightly above the entanglement threshold, at  $\Phi = 0.22\%$  (w/w),  $L_e(\text{optimum})$  must be somewhat less than 150 nm, since  $M_e \sim 1/\Phi$ .

Based on this, we postulate that for electrophoretic separations in dilute HEC solutions  $L_e$  must be comparable and perhaps a bit larger than restriction fragment contour length in order to give fine resolution. Referring to Table II

TABLE II  
THE MOLECULAR CONTOUR LENGTH BETWEEN ENTANGLEMENT POINTS AT  $\Phi = \Phi^*$

$M_n$  = Number-average molecular weight of HEC.  
 $L_e$  = The contour length between entanglement points.

$M_n$	$\Phi^*$ (% (w/w))	$L_e(\Phi^*)$ (nm)
27 000	1.80	25.7
35 900	1.25	34.2
63 800	0.68	60.7
105 000	0.37	100.1
160 000	0.21	152.5
306 000	0.11	292.1
438 800	0.09	417.6

again, consider  $L_e(\Phi^*)$  for  $M_n$  105 000 HEC. Since for this polymer,  $L_e(\Phi^*) \approx 100$  nm, shorter than the postulated  $L_e(\text{optimum})$  of about 150 nm,  $M_n$  105 000 HEC concentration must be less than  $\Phi^*$  [0.37% (w/w)] for separation of the 271/281 bp fragments, as is the case for HEC smaller than  $M_n$  105 000. Since for  $M_n$  160 000,  $M_n$  306 000, and  $M_n$  438 800 HEC,  $L_e$  is too large to provide separation of 271/281 bp fragments at the entanglement threshold, these polymers must all be at a concentration greater than their entanglement thresholds in order to reach the optimum  $L_e$ ; and the larger  $L_e(\Phi^*)$  is, the further the solution must be past  $\Phi^*$ .

We propose a tentative explanation for the finding. If  $L_e$  is a great deal shorter than the contour length of the DNA, then the probability that the DNA will form a strong entanglement with that loop in the HEC network is small, since this will not present a significant hindrance to the DNA motion. At the other extreme, if the HEC loop between two entanglement points is much larger than the contour length of the DNA, the smaller DNA molecule will have a high probability of passing through the loop easily without becoming entangled. Therefore, in order for strong entanglement interactions to occur between a DNA fragment and a given

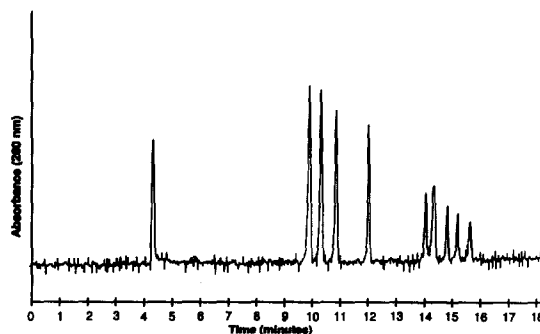


Fig. 11. Capillary electrophoresis of  $\Phi$ X174/*Hae*III restriction fragments ranging in size from 72 to 1353 bp in 0.12% (w/w)  $M_n$  438 800 HEC, 89 mM Tris-89 mM boric acid-5 mM EDTA. Reading from left to right (not including the first peak, which is a marker), the species are 1353, 1078, 872, 603, 310, 281 + 271, 234, 194, 118 + 72 bp in length, respectively. Conditions: field strength 221.4 V/cm; current 7.1  $\mu$ A; UV detection at 260 nm; capillary dimensions, 50 cm total length (35 cm to detector)  $\times$  51  $\mu$ m I.D.; temperature, 30  $\pm$  0.1°C. R.S.D. of absolute electrophoretic mobilities: 0.54%,  $n = 3$ .

HEC loop formed between entanglement points, they must be of comparable length. And since HEC is more flexible than DNA in solution, perhaps the HEC must be a bit longer in order to present enough resistance to hang up the DNA.

Another finding of interest is that the largest HEC molecular weight,  $M_n$  438 800, resolved the largest  $\Phi$ X174/*Hae*III restriction fragments quite easily (Fig. 11), and *could* resolve still larger fragments. In fact, if larger HEC were used, perhaps DNA restriction fragments which are quite large (>20 000 bp) could be separated with uncross-linked cellulosic polymers. Work is proceeding in our laboratory to confirm this prediction.

## CONCLUSIONS

We have shown that, theoretically, an entanglement coupling interaction between HEC molecules and DNA molecules during electrophoresis is capable of imparting a strong size-dependence to the electrophoretic mobility of the DNA by altering its frictional characteristics. We suggest, therefore, that this is the mechanism by which DNA is separated in uncross-linked HEC solutions.

We have correlated the entanglement threshold of HEC molecules with number-average molecular weight, and shown that  $\Phi^* \approx N^{-1.2}$ , a scaling dependence which is not compatible with the predictions of either deGennes [19] or Bueche [16]. The reason for this incompatibility is probably related to the fact that HEC is stiff and extended in solution. As such, it exhibits the effects of entanglement coupling to a larger degree than the highly flexible, random coil-like polymers for which these theories were derived. We have presented a relationship which allows calculation of the observed entanglement threshold for any HEC sample in water, given that the number-average molecular weight is known or can be estimated.

We have demonstrated that a fully entangled network of uncross-linked HEC is not necessary for separation of DNA restriction fragments by electrophoresis (*i.e.*, the HEC solution can be significantly below its entanglement threshold).

It is highly unlikely that the mechanism of separation in this case is the same as that applicable to the semi-rigid, porous network of a cross-linked gel.

Furthermore, we have shown that using uncross-linked HEC with a number-average molecular weight greater than 105 000, it is possible to separate restriction fragments that differ by only 10 base pairs. Our experiments show that for four different HEC molecular weights, the optimum concentration for separating these two restriction fragments is the same [0.22% (w/w) HEC], regardless of the length of the HEC. These findings support the assertion that beyond the entanglement threshold, the distance between entanglement points is independent of molecular weight and dependent only on concentration. We have used the concept of the average contour length between entanglements to infer that the optimum distance between HEC entanglements to separate a given mixture of restriction fragments is comparable to the average contour length of the DNA fragments in solution.

Based on this mechanism, there is no obvious limit to the size of the DNA which can be separated by this entanglement coupling between the DNA and uncross-linked polymers in solution.

## ACKNOWLEDGEMENTS

We thank Maria Helen Kleemiss at the Max-Planck-Institut für Kohlenforschung for helpful discussions.

## REFERENCES

- 1 M. Strega and A. Lagu, *Anal. Chem.*, 63 (1991) 1233.
- 2 H.E. Schwartz, K. Ulfelder, F.J. Sunzeri, M.P. Busch and R.G. Brownlee, *J. Chromatogr.*, 559 (1991) 267.
- 3 D.N. Heiger, A.S. Cohen and B.L. Karger, *J. Chromatogr.*, 516 (1990) 33.
- 4 P.D. Grossman and D.S. Soane, *Biopolymers*, 31 (1991) 1221.
- 5 A.M. Chin and J.C. Colburn, *Am. Biotech. Lab.*, 7 (1989) 16.
- 6 P. Bocek and A. Chrambach, *Electrophoresis*, 13 (1992) 31.

- 7 A. Chrambach and A. Aldroubi, *Electrophoresis*, 14 (1993) 18.
- 8 M. Chiari, M. Nesi, M. Fazio and P.G. Righetti, *Electrophoresis*, 13 (1992) 690.
- 9 H. Pulyaeva, D. Wheeler, M.M. Garner and A. Chrambach, *Electrophoresis*, 13 (1992) 608.
- 10 W. Brown, *Ark. Kemi*, 18 (1961) 227.
- 11 J.D. Ferry, *Viscoelastic Properties of Polymers*, Wiley, New York, 3rd ed., 1980.
- 12 P.R. Saunders, D.M. Stern, S.F. Kurath, C. Sakoontim and J.D. Ferry, *J. Colloid Sci.*, 14 (1959) 222.
- 13 F. Bueche, *J. Polym. Sci.* 25 (1957) 243.
- 14 C.R. Cantor and P.R. Schimmel, *Biophysical Chemistry, Part III: The Behavior of Biological Macromolecules*, Freeman, New York, 1980.
- 15 A. Einstein, *Ann. Physik*, 17 (1905) 549.
- 16 F. Bueche, *Physical Properties of Polymers*, Wiley, New York, 1962.
- 17 T.G. Fox and S. Loshaek, *J. Appl. Phys.*, 26 (1955) 1080.
- 18 H.R. Allcock and F.W. Lampe, *Contemporary Polymer Chemistry*, Prentice-Hall, Englewood Cliffs, NJ, 1981.
- 19 P.G. deGennes, *Scaling Concepts in Polymer Physics*, Cornell University Press, Ithaca, NY, 1979.
- 20 J. Brandrup and E.H. Immergut, *Polymer Handbook*, Wiley, Ithaca, 1989.
- 21 J.D. Ferry, *Viscoelastic Properties of Polymers*, Wiley, New York, 1st ed., 1961.
- 22 P.R. Sperry, *J. Colloid Interface Sci.*, 87 (1982) 375.
- 23 P.D. Grossman, J.C. Colburn and H.H. Lauer, *Anal. Biochem.*, 179 (1989) 28.
- 24 F. Rodriguez, *Principles of Polymer Systems*, Hemisphere Publishing, New York, 1989.
- 25 J. Beebe-Poli and M.R. Schure, *Anal. Chem.*, 64 (1992) 896.